MEC E 539
Assignment 4: Laminar flow Around a Square Object

by: Alex Diep

Date: March 28, 2023

CCID: abdiep
Student ID: 1664334

Contents

List of Figures

List of Tables

1 Problem Statement

1.1 Objective

The problem objective is to calculate the drag coefficient C_d of a square object at a Reynolds number of 20 and estimate the length of a vortex that forms behind the object.

Secondary objectives include learning about mesh refinement and mesh convergence. The problem will be solved numerically in ANSYS Fluent for five systematically refined meshes. The first (coarsest) mesh should contain in the order of 2000-3000 cells or control volumes with a cell size of 5.0 mm. The rest of the meshes are generated by reducing the size of each cell by two in both directions, i.e. increasing the total number of cells by four. The topology of the mesh remains the same as the mesh is refined. During the simulation, it is necessary to monitor the drag force F_d as a function of iteration.

The working fluid is air, with the properties given in Table 1.

Table 1: Fluid Properties

Property	Value
Density, ρ	1.0 kg/m^3
Dynamic Viscosity, μ	2.0×10^{-5} kg/m·s

1.2 Mathematical Model

1.2.1 Flow Description

For the mathematical description of fluids, the Navier-Stokes equations are an appropriate description of the flow. The continuity equation is given by

$$\frac{\partial}{\partial t}(\rho\vec{v}) + \nabla \cdot (\rho\vec{v}\vec{v}) = 0$$

the momentum equation is

$$\frac{\partial}{\partial t}(\rho\vec{v}) + \nabla \cdot (\rho\vec{v}\vec{v}) = -\nabla p + \frac{1}{3}\mu\nabla(\nabla \cdot \vec{v}) + \mu\nabla^2\vec{v} + \rho\vec{b}$$

There are some simplifications that can be made to the Navier-Stokes equations. Noting that the Reynolds number is low (Re $\ll$ 100), the unsteady and convective terms can be neglected.

The flow is also incompressible, so the density is constant. The continuity equation simplifies to

$$\boxed{\nabla \cdot \vec{v} = 0}$$

The momentum equation simplifies to

$$\boxed{\mu \nabla^2 \vec{v} - \nabla p + \rho \vec{g} = 0}$$

1.2.2 Boundary Conditions

The boundary conditions for the problem are listed in Table 2.

Table 2: Boundary Conditions

Boundary	Condition
Inlet	$u\|_{\text{inlet}} = U_\infty = 0.04$ m/s
Outlet	$\left.\dfrac{\partial u}{\partial x}\right\|_{\text{outlet}} = 0$
Top and Bottom Walls	$\mu \left.\dfrac{\partial u}{\partial y}\right\|_{\pm 10D} = 0$
Square Wall	$\vec{v}\|_{\text{square}} = 0$

1.3 Computational Model Parameters

1.3.1 Geometry and Mesh

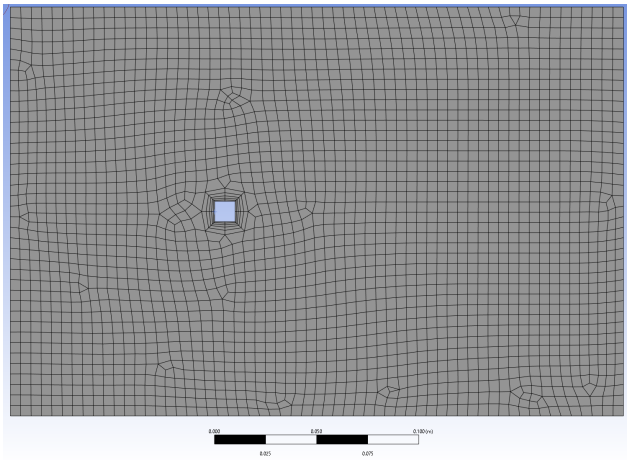

Figure 1: Geometry and Mesh for Mesh 1

The geometry of the simulation domain is a square object with side length $D = 0.01$ m. The domain is 0.2 m long and 0.1 m tall.

Face sizing was used with 5 inflation layers around the square with a growth rate of 1.2 and a default transition ratio of 0.272. The number of elements in each mesh is shown in Table 3. The mesh for the first mesh is shown in Figure 1.

Table 3: Mesh Sizes

Mesh	Element Size (mm)	Number of Elements
1	5.0	2390
2	2.5	9390
3	1.25	37870
4	0.625	152044
5	0.3125	613378

1.3.2 Boundary Conditions

First U_∞ needs to be determined. The Reynolds number is given from the problem statement as $Re = 20$. Then,

$$\text{Re} = \frac{U_\infty \rho D}{\mu}$$
$$\implies U_\infty = \frac{\text{Re}\mu}{\rho D}$$

The properties of air are given as $\rho = 1.0$ kg/m^3 and $\mu = 2.0 \times 10^{-5}$ kg/m·s. The side length of the square object is $D = 0.01$ m. Thus,

$$U_\infty = \frac{20 \times 2.0 \times 10^{-5}}{1.0 \times 0.01} = 0.04 \text{ m/s}$$

The inlet velocity was specified as $U_\infty = 0.04$ m/s. The outlet boundary condition was specified as zero pressure gradient. The top and bottom walls were specified as no-shear walls. The square wall was specified as a no-slip wall.

1.3.3 Solver Details

The solver details are shown in Table 4.

Table 4: General Solver Details

Type	Pressure Based
Velocity Formation	Absolute
Time	Steady
2D Space	Planar

The convergence criteria for continuity, x-velocity, and y-velocity were set to 10^{-5}. The spatial discretization scheme is shown in Table 5. A coupled solver was used. The maximum number of iterations was set to 1000.

Table 5: Discretization Scheme

Variable	Scheme
Gradient	Least Squares Cell Based
Pressure	Second Order
Momentum	Second Order Upwind

2 Results analyses

2.1 Convergence of Simulations

The residuals had a convergence criteria of 10^{-5}. For all grids, the residuals converged before the maximum number of iterations (1000) was reached. The drag coefficient reached a steady value in all grids. Figures 2 to 16 show the residuals, drag coefficient, and velocity profile for each grid.

Table 6: Grid Convergence

Grid	Iterations	Drag Force
1	57	2.513×10^{-5}
2	53	2.182×10^{-5}
3	51	2.079×10^{-5}
4	51	2.050×10^{-5}
5	52	2.045×10^{-5}

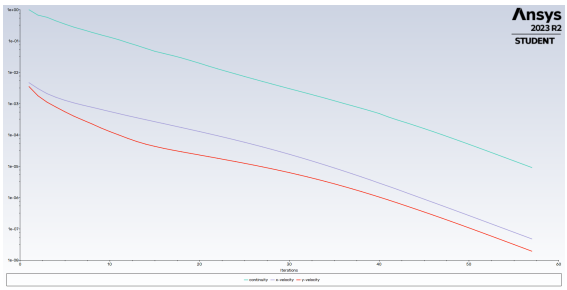

Figure 2: Residuals for Grid 1

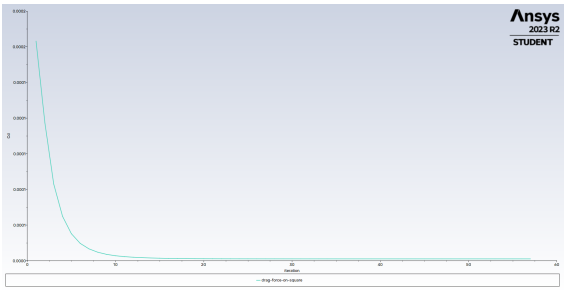

Figure 3: Drag Coefficient for Grid 1

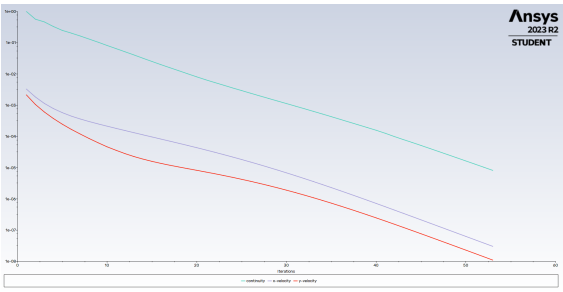

Figure 4: Residuals for Grid 2

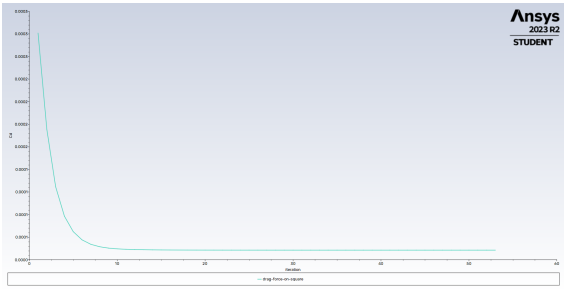

Figure 5: Drag Coefficient for Grid 2

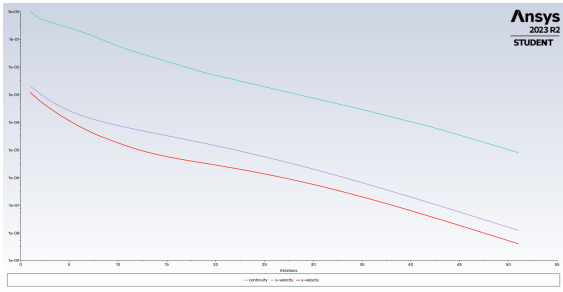

Figure 6: Residuals for Grid 3

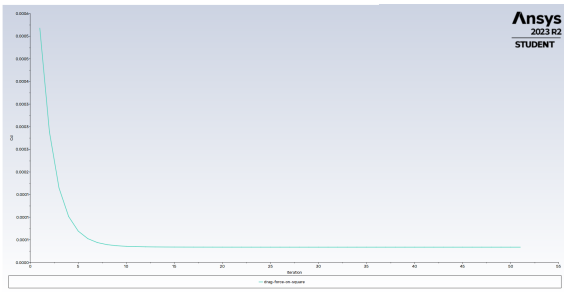

Figure 7: Drag Coefficient for Grid 3

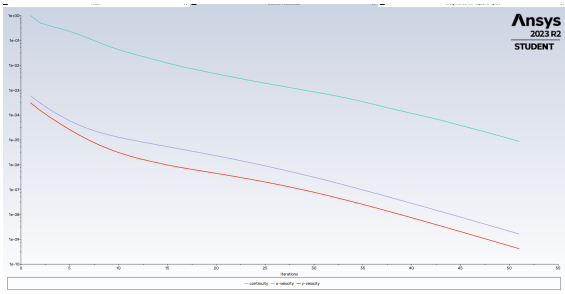

Figure 8: Residuals for Grid 4

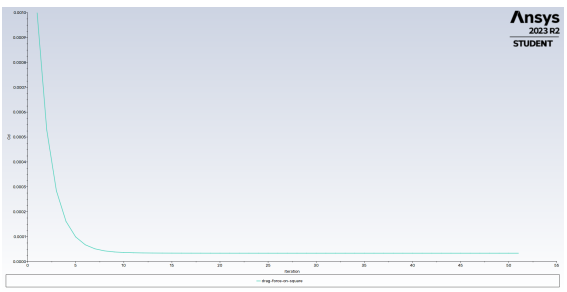

Figure 9: Drag Coefficient for Grid 4

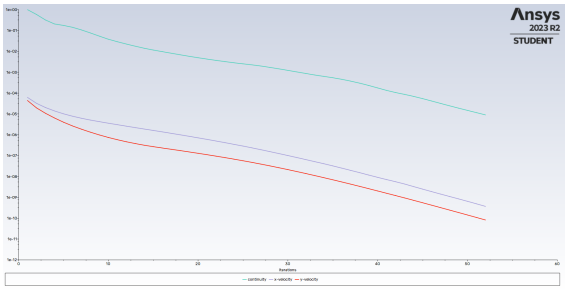

Figure 10: Residuals for Grid 5

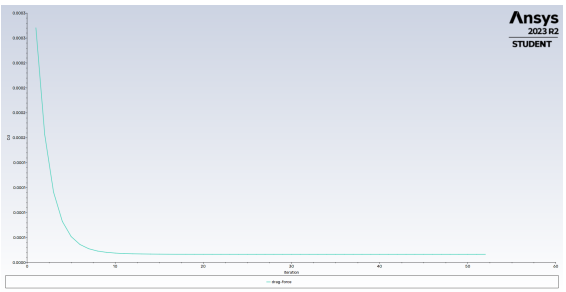

Figure 11: Drag Coefficient for Grid 5

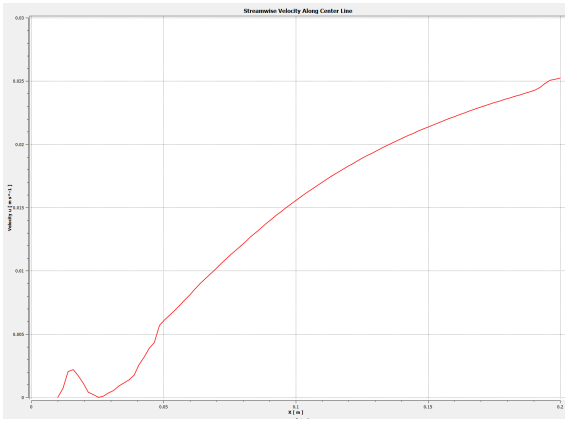

Figure 12: Velocity Profile for Grid 1

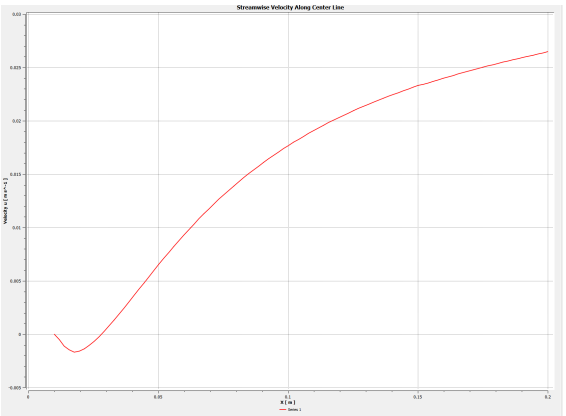

Figure 13: Velocity Profile for Grid 2

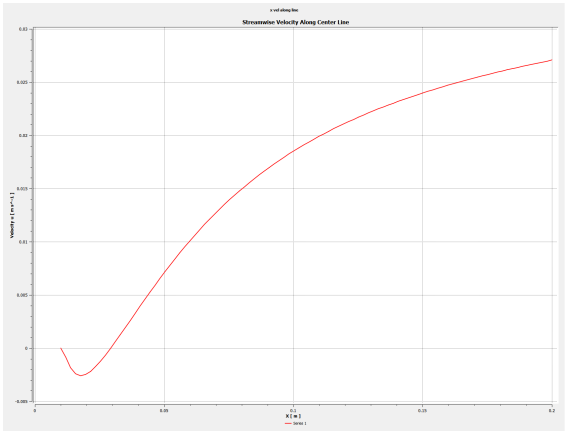

Figure 14: Velocity Profile for Grid 3

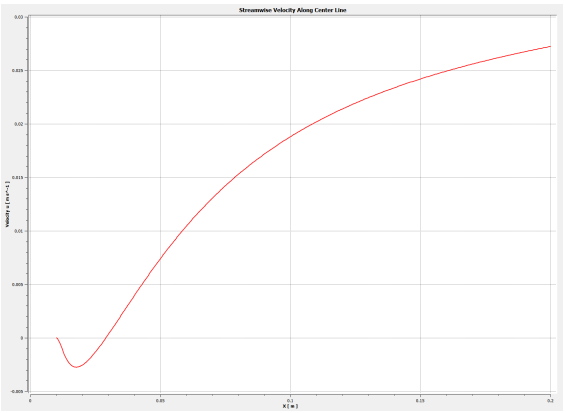

Figure 15: Velocity Profile for Grid 4

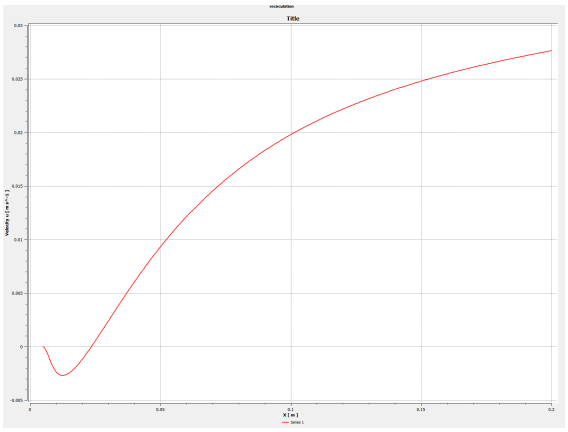

Figure 16: Velocity Profile for Grid 5

2.2 Analyses of the Velocity Fields

The contours are shown in Figures 17 and 18. The flow is symmetric about the centerline. The flow behind the square object is observable in grid 1, but much more refined in grid 5. In grid 5, two flanges of high velocity flow can be seen to the side of the square object. In comparison, the whole region to the side of the square object is a high velocity region in grid 1, which makes less physical sense. Grid 5 should be used since the results are more physical.

The streamlines are shown in Figures 19, 20, and 21. Again, the flow is symmetric about the centerline. A small vortex region can be seen from behind the square object in grids 3 and 5. The flow aspects are difficult to discern in grid 1. Considering that meshing grid 5 took roughly 20 minutes to mesh on my desktop computer, grid 3 is a good compromise between accuracy and computational cost.

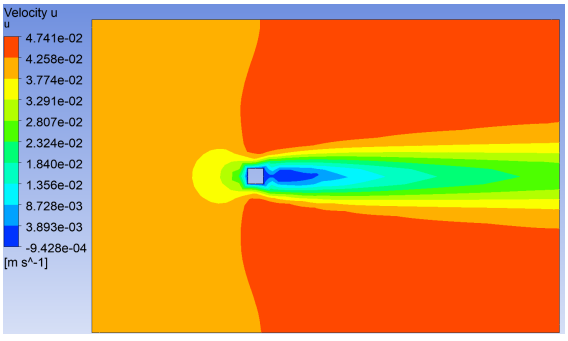

Figure 17: Velocity Contour for Grid 1

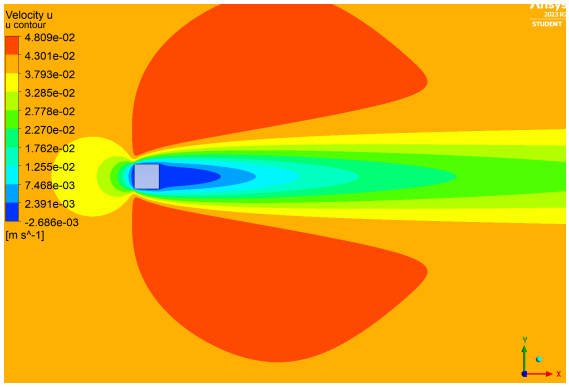

Figure 18: Velocity Contour for Grid 5

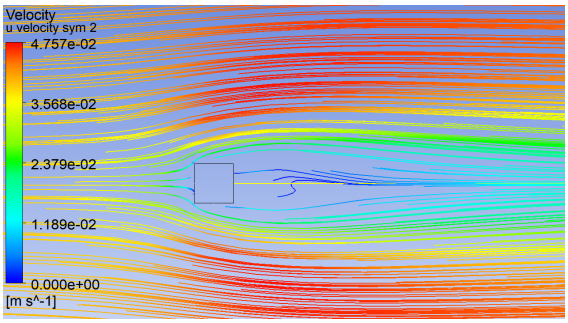

Figure 19: Streamlines for Grid 1

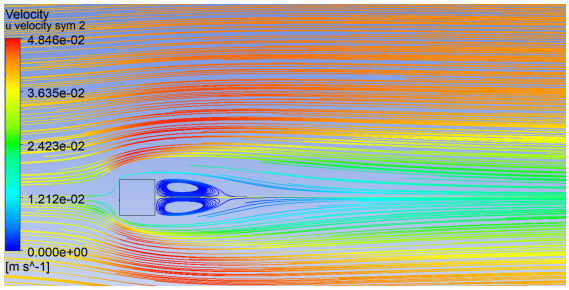

Figure 20: Streamlines for Grid 3

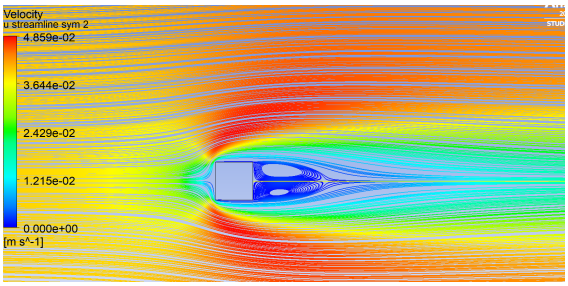

Figure 21: Streamlines for Grid 5

2.3 Drag Coefficient and Vortex Length

2.3.1 Vortex Length and Drag Coefficient

The vortex length and drag coefficient are summarized in Table 7.

Table 7: Vortex Length and Drag Coefficient

Grid	Recirculation Length (m)	Drag Coefficient
1	0.0115	3.1413
2	0.0181	2.7280
3	0.0186	2.5984
4	0.0183	2.5630
5	0.0183	2.5557

Sample calculations for grid 1 will be shown. The recirculation length is the distance between the two points (x_1, x_2) where the velocity is zero. Then

$$\begin{aligned} L_r &= x_2 - x_1 \\ &= 0.0234 - 0.0119 \\ &= 0.0115 \text{ m} \end{aligned}$$

The drag coefficient is calculated as

$$\begin{aligned} C_d &= \frac{2F_d}{\rho U_\infty^2 D} \\ &= \frac{2 \times 2.51 \times 10^{-5}}{1.0 \times 0.04^2 \times 0.01} \\ &= 3.1413 \end{aligned}$$

2.3.2 Recirculation Length on All Grids

The combined plot of the velocity profile for all grids is shown in Figure 22. Grid 1 does not really have a recirculation length, while grid 2 shows some recirculation. In Grids 3-5, asymptotic behavior is observed. The recirculation length seems to steady around grid 4, with grid 5 being almost indistinguishable. Grid 3 seems to capture the details of grids 4 and 5 for ˜16x fewer cells.

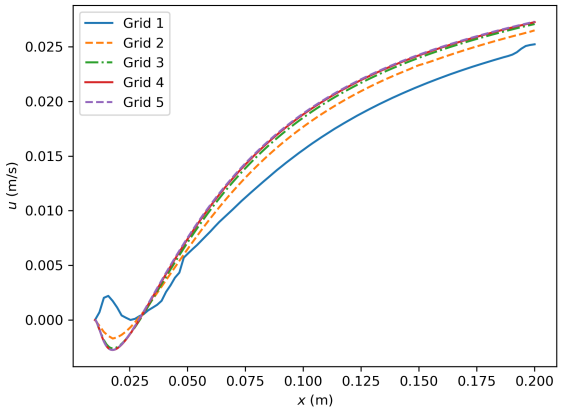

Figure 22: Velocity Profile for All Grids

2.3.3 Mesh Independence

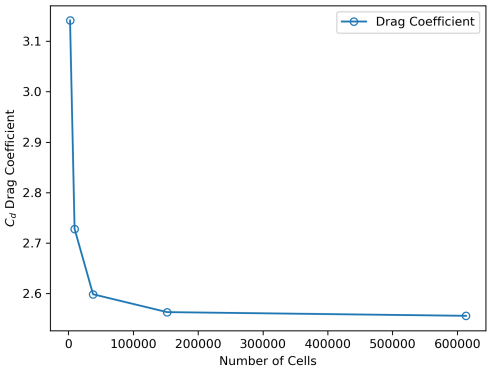

Figure 23: Drag Coefficient vs. Cells

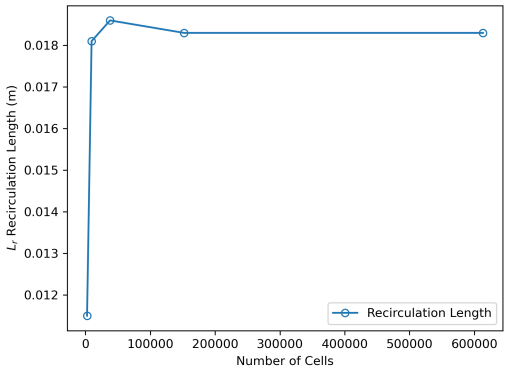

Figure 24: Recirculation Length vs. Cells

Table 8: Error in Vortex Length and Drag Coefficient with Respect to Grid 5

Grid	Vortex Length Error (%)	Drag Coefficient Error (%)
1	37.16	22.92
2	1.09	6.75
3	1.64	1.67
4	0	0.29
5	-	-

The drag coefficient and recirculation length are plotted against the total number of cells in Figures 23 and 24. Asymptotic behavior is observed in both plots. Grid 3 is within 1.6% of grid 5 for both the drag coefficient and recirculation length. The relative errors are summarized in Table 8.

2.4 Estimation of the Order of the Method

First calculate the order of the method. The order is calculated as

$$\begin{aligned} p &\approx \frac{\log\left(\frac{F_{\Delta x_4} - F_{\Delta x_3}}{F_{\Delta x_5} - F_{\Delta x_4}}\right)}{\log a} \\ &= \frac{\log\left(\frac{2.050 - 2.079}{2.045 - 2.050}\right)}{\log 2} \\ &= \boxed{2.268} \end{aligned}$$

This is close to the expected value of 2. Therefore, the Richardson extrapolation can be used to estimate the exact drag coefficient. The error in the drag coefficient is calculated as

$$\begin{aligned} \epsilon &= \frac{C_{\Delta x_5} - C_{\Delta x_4}}{a^p - 1} \\ &= \frac{2.5557 - 2.5630}{2^{2.268} - 1} \\ &= -0.001923 \end{aligned}$$

then,

$$\begin{aligned} C_{\text{exact}} &\approx C_{\Delta x_5} + \epsilon \\ &= 2.5557 - 0.001923 \\ &= \boxed{2.5537} \end{aligned}$$

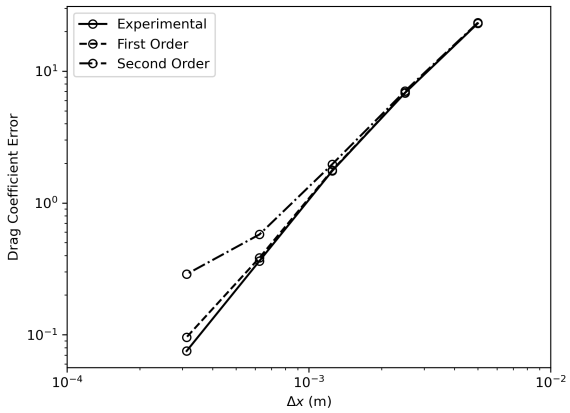

Figure 25: Error in Drag Coefficient vs. Element Size

The error in the drag coefficient against the element size is shown in Figure 25. The experimental error decreases faster than the first and second order lines. This is consistent

with the calculated order of the method being greater than 2. The data points from the experimental order and the second order are nearly coincident for the first 4 grids.

The order of convergence being higher than 2 is likely due to some phenomena in the meshing process that is not accounted for in the theoretical order of the method. Further work could be performed to determine the exact cause of the higher order of convergence.

2.5 Validation of the Results

From another study, the drag coefficient was found to be 1.5657 at a Reynolds number of 60 [1]. The drag coefficient was found to be 2.5537 at a Reynolds number of 20, which is the same order of magnitude. The relative error is then

$$\begin{aligned}\text{Relative Error} &= \frac{2.5537 - 1.5657}{1.5657} \\ &= \boxed{63.1\%}\end{aligned}$$

This is a large error, but the Reynolds number is three times smaller than the Reynolds number in the other study.

Since Reynolds number is low, this can be approximated as Stokes flow. Since density vanishes in Stokes flow, it can be shown from Buckingham Pi theorem that drag is a function of speed, length, and viscosity. Written mathematically,

$$F_d = C_1 \mu U_\infty D$$

where C_1 is a constant dependent on the geometry. The drag coefficient is then

$$\begin{aligned}C_d &= \frac{2F_d}{\rho U_\infty^2 D} \\ &= \frac{2C_1 \mu U_\infty D}{\rho U_\infty^2 D} \\ &= \boxed{\frac{C_2}{\text{Re}}}\end{aligned}$$

Thus, the drag coefficient is inversely proportional to the Reynolds number in Stokes flow. It is reasonable that the drag coefficient would be larger at a lower Reynolds number. The results are within the same order of magnitude, so the results are reasonable.

Note: I reran the simulation on grid 5 with Re = 60 and found the drag coefficient to be 1.6962, which is within 8.3% of the other study. This suggests that the error in the original simulation is due to the Reynolds number difference.

3 Conclusions

The results of the study found the drag coefficient on the square at Re= 60 for a mesh size of 0.3125 mm (613378 elements) to be $C_d = 2.5557$. This was compared to another study at Re= 20 which found $C_d = 1.5657$. The relative error was found to be 63.1%. The likely reason for this discrepancy is the difference in Reynolds number. The drag coefficient is expected to decrease with increasing Reynolds number, which is consistent with the observed results. An additional simulation at Re= 60 with grid 5 was conducted and found $C_d = 1.6962$, which is closer to the expected value.

The order of convergence was found to be 2.27, which is higher than the expected value of 2. This discrepancy may be due to the influence of other factors such as numerical errors, solver settings, or mesh quality. Further investigation is needed to identify the source of this discrepancy and improve the accuracy of the simulations.

Richardson extrapolation was used to estimate the drag coefficient at Re= 60 with an infinite number of elements. The estimated value was $C_d = 2.5537$, which is within 4.7% of grid 3.

The computation time to mesh the geometry grew exponentially with the number of elements. The time taken to mesh grid 5 was 1 hour on my peanut laptop, which was painful. The limitations of computer hardware and software were evident in this study, highlighting the need to balance computational resources with simulation accuracy.

Past grid 3, the drag coefficient was sufficiently accurate, and further mesh refinement would be unnecessary unless higher accuracy is required. A mesh with similar qualities to grid 3 will likely be the baseline mesh for future studies. It provides a good balance between accuracy and computational cost, making it suitable for most applications.

4 References

[1] A. Ostapenko and G. Bulanchuk, "Calculations of the drag coefficient of circular, square and rectangular cylinders using the lattice Boltzmann method with variable lattice speed of sound," *Afrika Matematika*, vol. 29, no. 1-2, pp. 137–147, Mar. 2018. [Online]. Available: http://link.springer.com/10.1007/s13370-017-0531-7